



Kinetic modeling of wet peroxide oxidation with a carbon black catalyst

J.L. Diaz de Tuesta, A. Quintanilla*, J.A. Casas, J.J. Rodriguez

Sección de Ingeniería Química, Universidad Autónoma de Madrid, Ctra. de Colmenar km 15, 28049, Madrid, Spain



ARTICLE INFO

Article history:

Received 15 November 2016

Received in revised form 3 March 2017

Accepted 9 March 2017

Available online 10 March 2017

Keywords:

Wet peroxide oxidation

Carbon black catalyst

Kinetic model

ABSTRACT

A kinetic model has been developed describing the rate of hydrogen peroxide consumption and target pollutant (phenol) degradation in CWPO with a commercial carbon black as catalyst. The model allows following the evolution of the oxidation by-products (up to 12) through a detailed reaction pathway. The kinetic parameters were obtained by fitting the experimental results in batch reactor runs at $T = 90\text{--}130^\circ\text{C}$, $P = 4\text{ bar}$, $[\text{Phenol}]_0 = 1\text{ g/L}$, $[\text{catalyst}] = 0\text{--}10\text{ g}_{\text{cat}}/\text{L}$ and the theoretical stoichiometric amount of hydrogen peroxide for complete mineralization of phenol (5 g/L). The results were subjected to the analysis of variance (ANOVA). The model includes a set of power-law expressions with different reaction orders which provides a complete description of the process and allows obtaining the efficiency of hydrogen peroxide consumption under giving operating conditions.

© 2017 Elsevier B.V. All rights reserved.

1. Introduction

Catalytic wet peroxide oxidation (CWPO) relies on the treatment of wastewater by oxidation of the organic pollutants with hydroxyl and hydroperoxy radicals, produced by the catalytic decomposition of hydrogen peroxide under circumambient to more severe operating conditions ($T = 25\text{--}130^\circ\text{C}$, $P = 1\text{--}5\text{ atm}$). It represents an emerging technology whose main challenge, currently limiting its industrial application, is the development of not only active but also stable solid catalysts capable of performing at efficient H_2O_2 consumption.

Current trends are addressing the development of bare carbon-based materials as CWPO catalysts, thus avoiding the presence of metallic phase susceptible of leaching [1,2]. Activated carbons are the most studied, mainly tested for the treatment of organic dyes [3–10]. Also, graphites [9,11,12] and to a lesser extent, carbon nanotubes, nanofibers and xerogels [9,12–14] have been used for the CWPO of phenol and derivatives. The work of Dominguez et al., [15] introduced the use of carbon black, viz. the Chemviron carbon black ($S_{\text{BET}} = A_{\text{ext}} = 75\text{ m}^2/\text{g}$, $C = 99\%$ and negligible ash content), as novel potential catalyst for this process. Its relative low specific surface area determines a low adsorption capacity hindering the formation of adsorbed oligomeric by-products on the carbon surface, respect to what occurs with activated carbons, and con-

sequently preventing deactivation. Complete conversion of phenol and around 70% TOC abatement were achieved in 24 h reaction time at 90°C and 5 g/L catalyst concentration using 1 g/L starting phenol concentration at initial pH 3.5. The remaining TOC corresponded to short-chain carboxylic acids. The efficiency of hydrogen peroxide consumption was maintained at 90–100% (ratio of TOC to H_2O_2 conversion, $X_{\text{TOC}}/X_{\text{H}_2\text{O}_2}$, percent).

Research on CWPO has been mainly focused on the development of highly active, stable and efficient solid catalysts and the kinetic studies reported are in general based on pseudo-first order rate equations describing the disappearance of target pollutants [16–25]. So far only a few works have been reported where crucial issues such as catalyst deactivation [26], homogeneous contribution [27], the existence of radical parasitic reactions [28,29] or the amount of specific active sites [30] have been considered.

The current work deals with the kinetic modeling of CWPO with a commercial carbon black as catalyst using phenol as target compound. Temperatures in the range $90\text{--}130^\circ\text{C}$ were tested. A model has been developed to follow the rate of phenol disappearance, hydrogen peroxide consumption, the evolution of the individual aromatic intermediates and acid by-products on the basis of the reaction pathway derived from the experimental results. Also, TOC evolution was predicted from the model.

* Corresponding author.

E-mail address: asun.quintanilla@uam.es (A. Quintanilla).

2. Materials and methods

2.1. Materials and reagents

Carbon black was supplied in powder form by Chemviron (ref.:2156090). Hydrogen peroxide solution (30% w/v) was purchased from Sigma-Aldrich. Working standard solutions of phenol, hydroquinone, resorcinol, catechol, *p*-benzoquinone, acetic acid, formic acid, malonic acid, maleic acid all from Sigma-Aldrich and oxalic acid (Panreac) were prepared and used for High Performance Liquid Chromatography (HPLC) and Ionic Chromatography (IC) calibration. Other reagents used in the analyses were H₂SO₄ (Panreac), Na₂CO₃ (Panreac), NaHCO₃ (Merck), TiOSO₄ (Riedel-deHaën). HCl (Panreac) or NaOH (Panreac) were used to adjust the initial pH of the reaction media. All these reagents were of analytical grade and were used without further purification. All solutions were prepared with milli-Q water.

2.2. CWPO experiments

The experiments were carried out in a stoppered glass batch reactor (Büchi, inertclave Type I) equipped with a backpressure controller. The reaction volume was 400 mL and the starting concentrations of reactants were 1 g/L phenol and 5 g/L H₂O₂ (which corresponds to the theoretical stoichiometric amount for mineralization of phenol). The catalyst was always the CWPO-second use carbon black. In a previous study [15], it was observed that the activity, tested in five consecutive runs of 24 h each, increased from the first to the second use and then remained almost unchanged. This increase was attributed to the higher hydrophilicity and electrochemical capacity of the use carbons as a consequence of the increased population of surface oxygen groups upon the first 24 h of CWPO reaction (mainly carboxylic acid and, in less extent, anhydride, ether and phenol moieties). Thus, the as-received catalyst in the current study was previously used in CWPO during 24 h under identical operating conditions to those used in the subsequent runs.

Initially, 370 mL of milli-Q water with the selected amount of carbon black was placed into the reactor and the mixture stirred. A N₂ flow rate of 100 mL/min was used to achieve the selected pressure and temperature. Then, 10 mL of 40 g/L phenol solution and 20 mL of an adjusted solution of hydrogen peroxide were injected, being this the starting time for the reaction. The pressure was maintained at 4 atm during the reaction by means of a back-pressure control valve. The temperature was tested within the 90–130 °C range and the catalyst concentration within 0–10 g/L. The initial pH value was ranged from 3.5 to 10.5 and not controlled along the process. Samples at different reaction times were taken from the reactor. The catalyst was separated by filtration (0.45 µm Nylon filter) and the sample was immediately cooled and analyzed.

2.3. Analytical methods

Phenol and aromatic intermediates were analyzed by HPLC (Varian, Mod. ProStar) using a 5 µm FORTIS C18 column (150 × 4.6 mm) with a mixture of 4 mM H₂SO₄ aqueous solution at 1.3 mL/min as mobile phase. A diode array detector (PDA) at wavelengths of 210 and 246 nm was used. Short-chain organic acids were determined by ionic chromatography (Metrohm, mod. 883 BASIC IC Plus) with anionic chemical suppression using a conductivity detector. A Metrosep A supp 5–250 column (25 cm length, 4 mm diameter) was used as stationary phase and 0.7 mL/min of an aqueous solution 3.2 mM of Na₂CO₃ and 1 mM of NaHCO₃ as mobile phase. Total Organic Carbon (TOC) was measured with a TOC analyzer (Shimadzu TOC VSCH). Hydrogen peroxide concentration was determined by colorimetric titration with a UV2100 Shimadzu

UV-vis spectrophotometer using the TiOSO₄ colorimetric method [31].

2.4. Kinetic modeling

The production rate of each given compound (*i*) in the reaction medium, R_i (mol·g_{cat}⁻¹·s⁻¹), is given by:

$$R_i = \frac{d[i]}{[W] \cdot dt} \quad (1)$$

where the terms in brackets refer to the concentrations of *i* (mol·L⁻¹) and catalyst (W, g·L⁻¹). R_i can be expressed as a function of the concentration of the species involved in the reaction according to the corresponding pathway.

The numerical integration of the rate equations in a batch reactor with the initial conditions [Phenol] = [Phenol]₀, [H₂O₂] = [H₂O₂]₀ and [reactor products] = 0 at t = 0 was solved by using the Microsoft Excel Solver (Microsoft Office 2010, Microsoft Corp.) based on the Generalized Reduced Gradient (GRG) algorithm for least squares minimization. The equations were solved at each temperature. The activation energy and the pre-exponential factor values were calculated using the Arrhenius equation.

Analysis of variance (ANOVA) was used for statistical model evaluation. The F-value and the critical F-value were calculated in order to compute the statistical significance of the regressions. The F-value is the ratio of the mean square due to regression to mean square due to error. The critical F-value was obtained from the F-distribution for a significance level of 0.05. The computed F-values should be several times greater than the critical F-value for good agreement with the experimental data. The coefficient of determination (R^2) was also calculated by regression analysis of the experimental data.

3. Results and discussion

Kinetic control was verified under the operating conditions tested. Both, the catalyst in powder form (42 nm) and the appropriate stirring velocity (300 rpm) were used to avoid mass transfer limitations.

Neutral initial pH was selected since a slight effect was observed when this variable was varied within the range from 3.5 to 10.5 (see Fig. S1 of Supporting Information).

Fig. 1 depicts the time-course of hydrogen peroxide, phenol and TOC upon 6 h of reaction, at different temperatures and catalyst loadings. As expected, higher H₂O₂, phenol and TOC conversions were achieved at increasing catalyst concentration. The observed initial rates increased linearly with that concentration (see Fig. S2 of Supporting Information).

A higher temperature increases the rate of H₂O₂ decomposition into active radical species (HO[•] and HOO[•]) [32], as the enhanced rate of phenol disappearance and mineralization indicate in the current study. Under 10 g/L catalyst and 130 °C, complete phenol disappearance and 80% TOC removal was achieved in 4 h reaction time. The trend in the TOC curve suggests the existence of some refractory by-products even under the most severe conditions.

3.1. Phenol oxidation route

The reaction by-products identified along the experiments of Fig. 1 were aromatic compounds, *viz.* resorcinol (RS), catechol (CTL), hydroquinone (HQ) and *p*-benzoquinone (BQ) and carboxylic acids, *viz.* maleic (MAL), fumaric (FUM), malonic (MLO), oxalic (OXA), acetic (ACE) and formic (FORM). The time-course of those species under the different conditions tested is shown in Figs. 2–4. The trend of the curves show that the aromatics and the C₃–C₄ carboxylic acids were intermediate compounds whereas formic, acetic

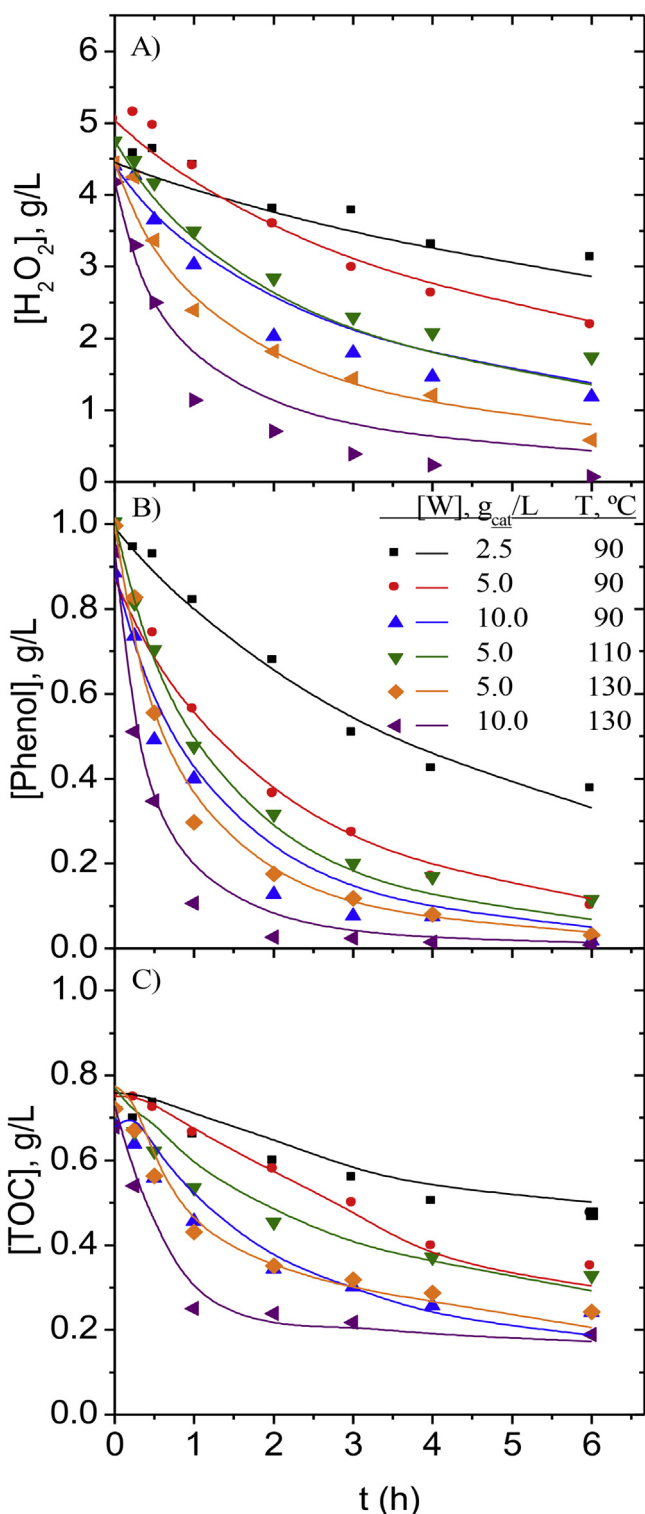


Fig. 1. Experimental (symbols) and predicted (curves) time-course of H_2O_2 , phenol and TOC under the different conditions tested.

and oxalic acids appear refractory to CWPO under the conditions tested, except the last one at the highest temperature and catalyst loading. Effective removal of the highly toxic aromatic intermediates within the 6 h of the experiments required working under those conditions.

On the other hand, the TOC values calculated from the identified by-products differed from the experimentally measured. This unidentified carbon is assigned to condensation products (CP).

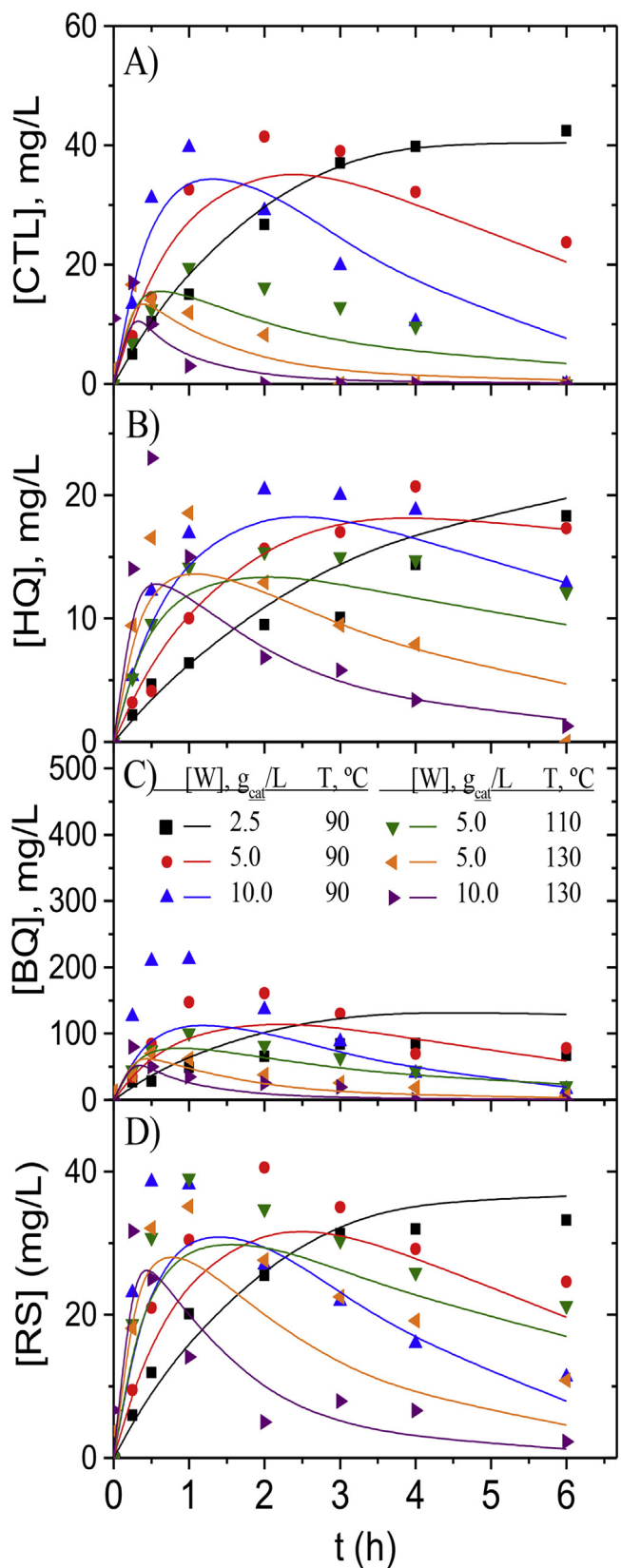


Fig. 2. Experimental (symbols) and predicted (curves) time-course of aromatic by-products under the different conditions tested.

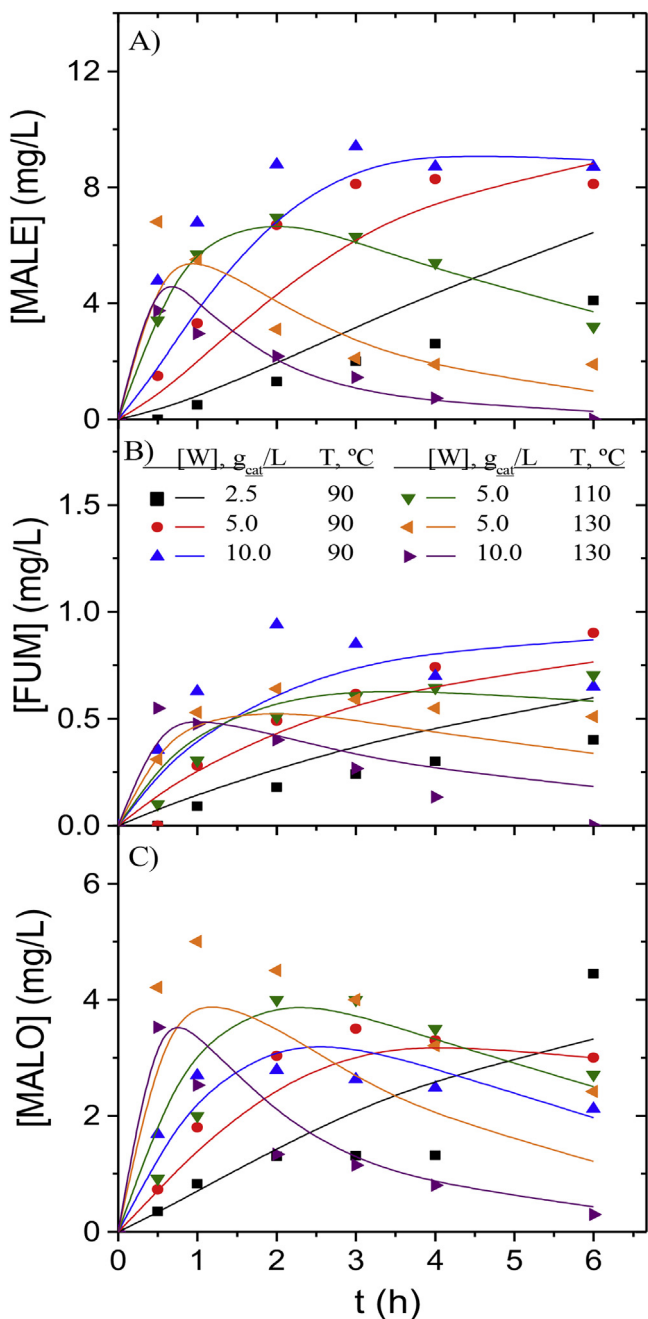


Fig. 3. Experimental (symbols) and predicted (curves) time-course of maleic, fumaric and malonic acids under the different conditions tested.

These species, already reported in wet oxidation studies using carbon catalysts [15,33–36], are considered oligomers from phenol oxidative coupling reactions taking place on the carbon surface. The time-course of the unidentified species in terms of equivalent carbon is depicted in Fig. 5. As observed, these condensation products are refractory to oxidative degradation under all the operating conditions tested, contributing along with formic and acetic acids to the residual TOC of the effluent. The oxidative coupling reactions are favored at low pH and high temperatures [37,38] which explains the increasing concentration with temperature.

3.2. Kinetic model

From the results of Figs. 1–5, the generalized reaction pathway of Fig. 6 is proposed.

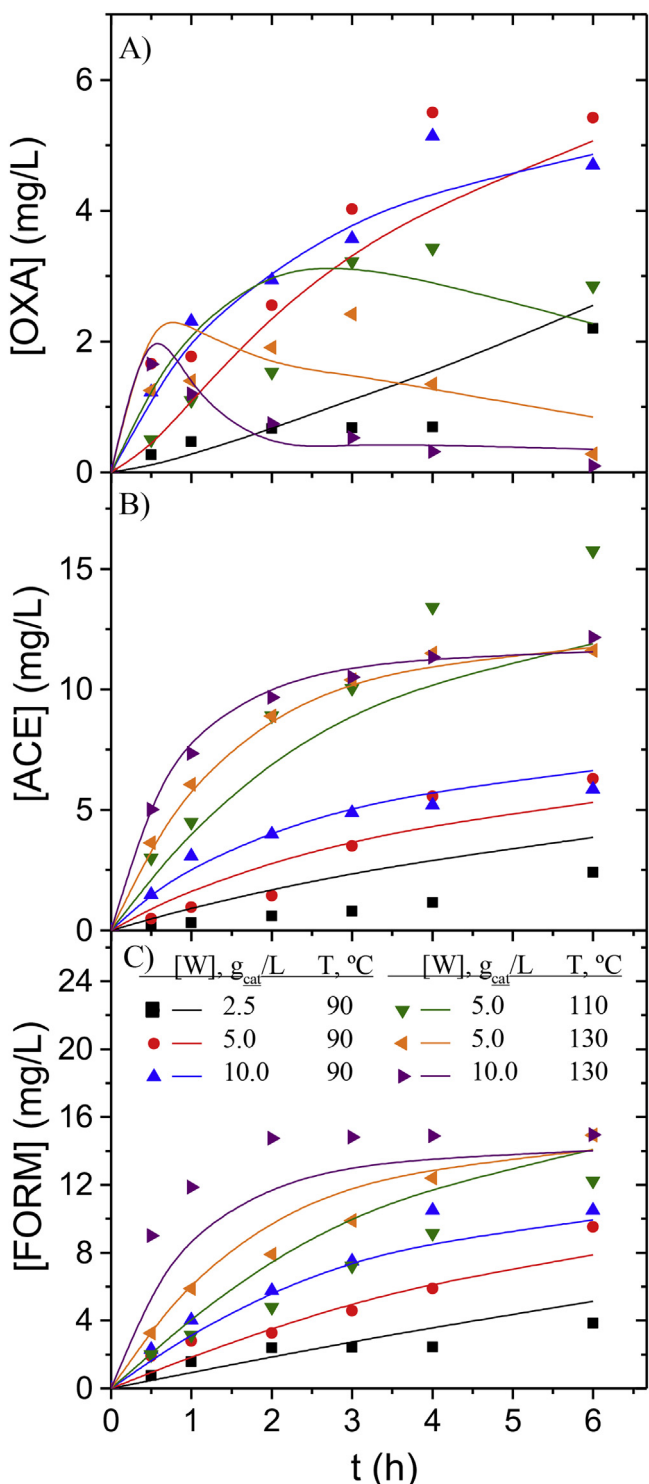
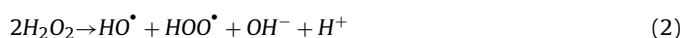


Fig. 4. Experimental (symbols) and predicted (curves) time-course of acetic, oxalic and formic acids under the different conditions tested.

Regarding hydrogen peroxide, it is known that it yields hydroxyl and hydroperoxy radicals on the carbon surface and these radicals further react with the organic matter. Thus, hydrogen peroxide disappearance can be described by the reaction:



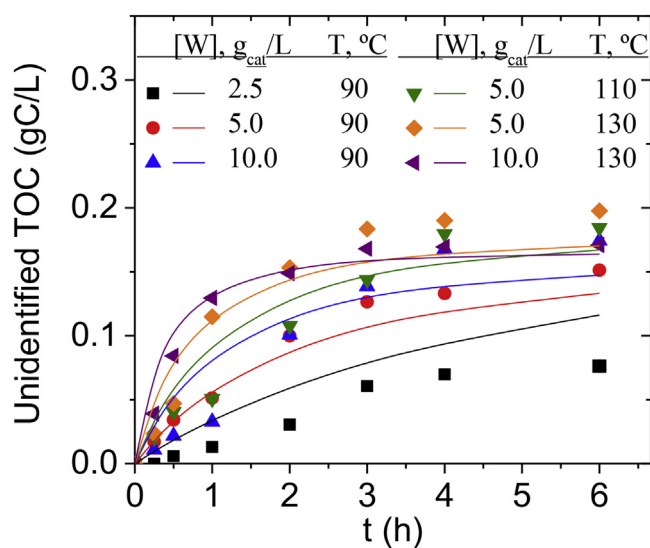
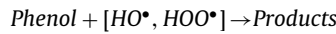


Fig. 5. Experimental (symbols) and predicted (curves) time-course of unidentified reaction products as equivalent C ($\text{TOC}_{\text{measured}} - \text{TOC}_{\text{calculated}}$) under the different conditions tested.

In case of phenol, an overall reaction has been considered by lumping all the by-products:



(3)

Simple power-law rate equations, of first or second reaction order with respect to each reactant as well as hyperbolic rate equations have been checked for H_2O_2 consumption and phenol degradation. Upon fitting to the experimental results of H_2O_2 and phenol concentration vs time (Fig. 1), the second order rate equation for H_2O_2 and first order to each reactant for phenol were statistically discriminated. The ANOVA analysis and the kinetic parameters obtained are summarized in Table 1. As can be seen, the F criterion (F -values > critical F -values) permits to validate the models and the R^2 values are indicative of the fitness. The highest deviation between the experimental and predicted values is observed at 130 °C and 10 g/L of catalyst. Under those operating conditions, the uncertainty of the model increases since the contribution of the homogeneous reaction becomes of some significance (higher than 30% of the overall phenol oxidation).

The production rates of aromatic by-products were expressed according to the different pathways. Considering their production from phenol in parallel reactions and their further oxidation. First-order rate equations with respect to both the organic species and hydrogen peroxide were assumed:

$$\frac{d[\text{arom} = \text{HQ}, \text{BQ}, \text{CTL}, \text{RSL}]}{[W] \cdot dt} = S_{\text{Ph} \rightarrow \text{arom}} \cdot k_{\text{Ph}} \cdot [\text{Ph}] \cdot [H_2\text{O}_2] - k_{\text{arom}} \cdot [\text{arom}] \cdot [H_2\text{O}_2] \quad (4)$$

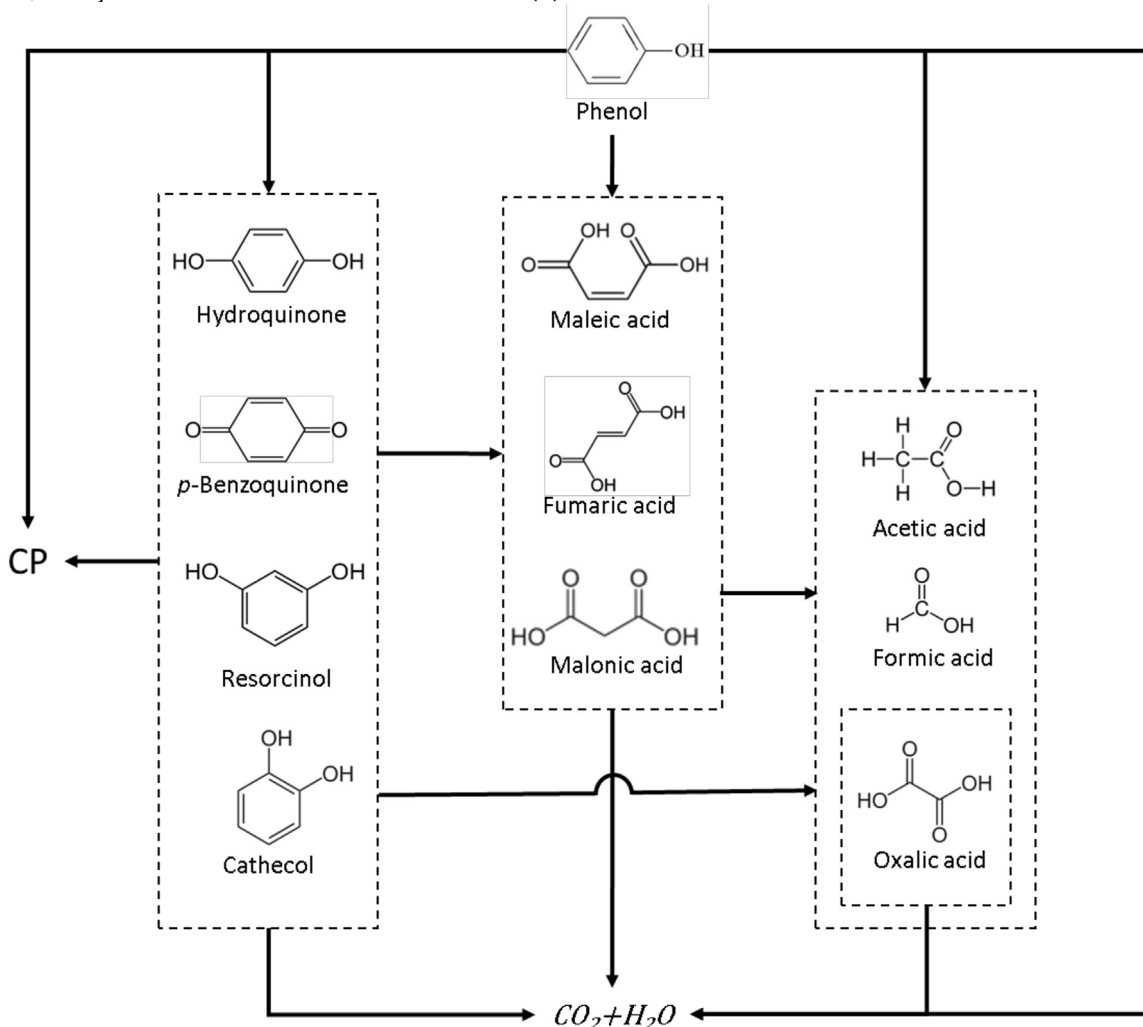


Fig. 6. Reaction pathway of phenol CWPO with carbon black catalyst.

Table 1

Statistical analysis of the kinetic equations checked for CWPO of phenol and values obtained for the apparent activation energy and pre-exponential factor.

Specie	F [§]	R ²	SSR (mg ² /L ²)	Ea (kJ/mol)	k ₀ (L ² mol ⁻¹ s ⁻¹ g _{cat} ⁻¹)
H ₂ O ₂	1913	0.98	3212	43 ± 10	131.7 ± 1.8 [¥]
Phenol	3757	0.99	69730	35 ± 3	21.0 ± 0.2 [¥]
HQ	125.1	0.95	264	66 ± 21	(2.36 ± 0.04) · 10 ⁵
BQ	27.3	0.81	54201	70 ± 9	(3.59 ± 0.002) · 10 ⁶
CTL	103.5	0.94	1497	86 ± 23	6.74 · 10 ⁸ ± 4.07 · 10 ³
RS	88.0	0.93	1582	48 ± 5	1700 ± 891
MALE	34.0	0.94	38.25	91 ± 22	1.00 · 10 ⁹ ± 3.99 · 10 ³
FUM	23.6	0.91	0.31	102 ± 30	1.31 · 10 ¹⁰ ± 5.27 · 10 ³
MALO	21.8	0.90	11.87	41 ± 6	200 ± 109
OXA	16.1	0.92	37.21	117 ± 12	3.01 · 10 ¹² ± 4.27 · 10 ³
ACE	95.6	0.98	7.62	—	—
FORM	53.4	0.96	83.41	—	—
CP	159	0.96	31051	—	—

[§] critical-F = 4.05 for H₂O₂ and phenol; 2.44 for TOC; 2.82 for aromatic species; 2.29 for acid species; 2.82 for C.P.

[¥] k₀ in (L² mol⁻² s⁻¹ g_{cat}⁻¹).

A S_{m → n} parameter, defined as the molar fraction of the m compound that converts into n, is included in order to estimate species distribution. It will be taken as constant within the catalyst concentration and temperature range tested.

In addition, another two set of equations have been considered attending to the simplified pathways proposed. One where hydroquinone and p-benzoquinone are lumped:

$$\frac{d[HQ + BQ]}{[W] \cdot dt} \cong S_{Ph \rightarrow (HQ+BQ)} \cdot k_{Ph} \cdot [Ph] \cdot [H_2O_2] - k_{HQ+BQ} \cdot ([HQ] + [BQ]) \cdot [H_2O_2] \quad (5)$$

$$\frac{d[arom = CTL, RS]}{[W] \cdot dt} = S_{Ph \rightarrow arom} \cdot k_{Ph} \cdot [Ph] \cdot [H_2O_2] - k_{arom} \cdot [arom] \cdot [H_2O_2] \quad (6)$$

and another lumping all the aromatics:

$$\frac{d[\sum arom = HQ + BQ + CTL + RS]}{[W] \cdot dt} = S_{Ph \rightarrow arom} \cdot k_{Ph} \cdot [Ph] \cdot [H_2O_2] - k_{\sum arom} \cdot [arom] \cdot [H_2O_2] \quad (7)$$

The experimental concentrations of the aromatic intermediates (Fig. 2) have been fitted to the integrated equations, with boundary conditions [intermediates] = 0 at t = 0, and taking into account the calculated concentrations of phenol and H₂O₂. The values of the kinetic parameters obtained with each model and the corresponding ANOVA results are summarized in Table S1 (provided in the

Supporting Information). The SSR value is significantly higher for the lumping model (Eq. (6)) and the best fitting for hydroquinone was obtained when it was not lumped with p-benzoquinone (Eq. (3)), as the higher F-values indicate (Table S1). Therefore, the discriminated model was that given in Eq. (3). The calculated concentration vs. time values for each species are given by the curves (lines) of Figs. 2. The values of apparent activation energy and pre-exponential factor together with the ANOVA results are included in Table 1. In general, the fittings are acceptable though the maximum concentrations are not always well predicted. The p-benzoquinone fitting being the poorest, with a factor of determination lower than 0.9 (Table 1), this could be in part attributed to the difficulty in quantifying this compound, due to its redox equilibrium with hydroquinone. To reduce this uncertainty, effluent samples were immediately analyzed. The activation energy values for the aromatic intermediates vary within the range of 48–86 kJ/mol, and they are higher than those obtained for phenol and hydrogen peroxide. The kinetic constants for the different compounds follow the order: k_{CTL} > k_{BQ} > k_{RS} > k_{HQ}.

The calculated S_{Ph → arom} values are given in Table 2. Hydroquinone is the most ecotoxic intermediate [39] but it has a minor presence since only 3% of phenol is oxidized to this compound. In contrast, 34% of phenol goes to p-benzoquinone (also quite ecotoxic) which is the intermediate reaching the highest concentration. Its relatively high oxidation rate allows achieving complete removal after 3 h at 130 °C and 10 g/L of catalyst. The sum of the S_{Ph → arom} values shows that 55 mol% of phenol is oxidized to aromatic intermediates.

Regarding to acid by-products, maleic, fumaric and malonic acids are produced upon oxidation of both phenol and aromatic

Table 2

Molar distribution of intermediates (S_{m → n}, %).

n species	m species									
	Phenol	RS	CTL	HQ	BQ	MALO	MALE	FUM	OXA	
RS	8.1	—	—	—	—	—	—	—	—	
CTL	9.5	—	—	—	—	—	—	—	—	
HQ	3.0	—	—	—	—	—	—	—	—	
BQ	34.4	—	—	—	—	—	—	—	—	
MALE	0.19	0.0	18.6	0.0	0.0	—	—	—	—	
FUM	0.06	0.3	0.0	1.9	0.01	—	—	—	—	
MALO	0.26	2.3	0.0	0.0	2.7	—	—	—	—	
OXA	0.0	9.5	0.0	0.0	0.0	0.0	0.0	0.0	—	
ACE	0.75	0.0	2.3	16.3	0.0	0.0	40	0.0	—	
FORM	0.90	14.3	0.0	0.0	0.0	100	0.0	100	—	
CP	24.6	0.0	0.0	0.0	0.0	—	—	—	—	
Total	81.8	26.4	20.9	18.2	2.7	100	40	100	0	
CO ₂ [§]	18.2	73.6	79.1	81.8	97.3	0.0	60	0.0	100	

[§] obtained by the direct mineralization of the m compound. Calculated as 100 – $\sum S_{m \rightarrow n}$ (%).

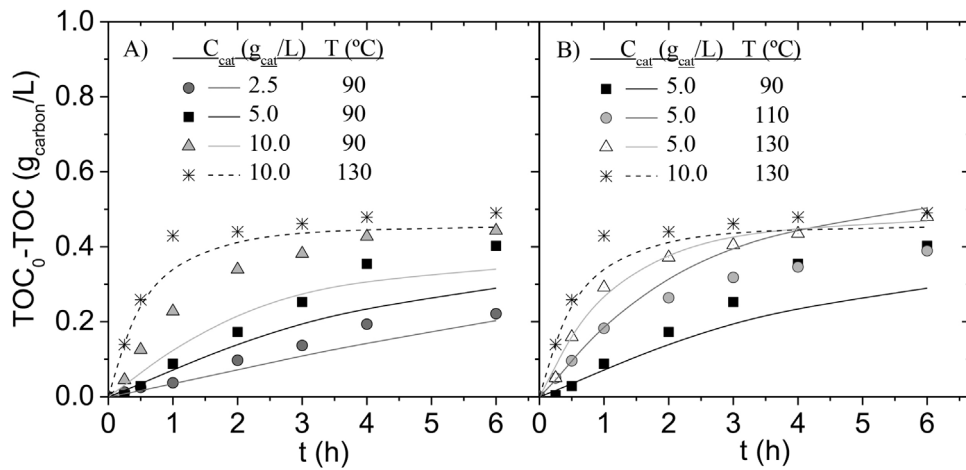


Fig. 7. Experimental (symbols) and predicted (curves) time-course of organic carbon evolved to CO_2 .

intermediates. Shorter-chain acids (viz. acetic, oxalic and formic) result also from the degradation of the heavier ones. Formic and acetic acids are refractory to further oxidation:

$$\frac{d[\text{acid} = \text{MALE}, \text{FUM}, \text{MALO}]}{[W] \cdot dt} = (S_{\text{Ph} \rightarrow \text{acid}} \cdot k_{\text{Ph}} \cdot [\text{Ph}] + \sum_{\text{arom.}=1}^4 S_{\text{arom} \rightarrow \text{acid}} k_{\text{arom}} \cdot [\text{arom}] - k_{\text{acid}} \cdot [\text{acid}] \cdot [\text{H}_2\text{O}_2]) \quad (8)$$

$$\frac{d[\text{OXA}]}{[W] \cdot dt} = (S_{\text{Ph} \rightarrow \text{OXA}} \cdot k_{\text{Ph}} \cdot [\text{Ph}] + \sum_{\text{arom.}=1}^4 S_{\text{arom} \rightarrow \text{OXA}} k_{\text{arom}} \cdot [\text{arom}] + \sum_{\text{acid}=1}^3 S_{\text{acid} \rightarrow \text{OXA}} \cdot k_{\text{acid}} \cdot [\text{acid}] - k_{\text{OXA}} \cdot [\text{OXA}] \cdot [\text{H}_2\text{O}_2]) \quad (9)$$

$$\frac{d[\text{ref.ac} = \text{FORM}, \text{ACE}]}{[W] \cdot dt} = (S_{\text{Ph} \rightarrow \text{ref.ac}} \cdot k_{\text{Ph}} \cdot [\text{Ph}] + \sum_{\text{arom.}=1}^4 S_{\text{arom} \rightarrow \text{ref.ac}} k_{\text{arom}} \cdot [\text{arom}] + \sum_{\text{ox.ac}=1}^3 S_{\text{acid} \rightarrow \text{ref.ac}} \cdot k_{\text{acid}} \cdot [\text{acid}] \cdot [\text{H}_2\text{O}_2]) \quad (10)$$

The values of apparent activation energy and pre-exponential factor together with the ANOVA results are summarized in Table 1. The F criterion (F -values > critical F -values) permits to validate

the models and the R^2 values (higher than 0.9) are indicative of the fitness. The calculated concentration vs. time values for each

species are given by the curves (lines) of Figs. 3 and 4. The fitting is quite acceptable, especially considering the low concentration values predicted. For instance, malonic and fumaric acids showed the poorest fitting, with a factor of determination around 0.9, and

Table 3
Kinetic modeling of phenol CWPO with carbon black as catalysts.

$$\begin{aligned} -\frac{d[\text{H}_2\text{O}_2]}{[W] \cdot dt} &= 131.7 \cdot \exp\left(\frac{-5172}{T}\right) \cdot [\text{H}_2\text{O}_2]^2 \\ -\frac{d[\text{Phenol}]}{[W] \cdot dt} &= 21.0 \cdot \exp\left(\frac{-4210}{T}\right) \cdot [\text{Phenol}] \cdot [\text{H}_2\text{O}_2] \\ \frac{d[\text{HQ}]}{[W] \cdot dt} &= \left[0.030 \cdot k_{\text{Ph}} \cdot [\text{Ph}] - 2.4E5 \cdot \exp\left(\frac{-7938}{T}\right) \cdot [\text{HQ}] \right] \cdot [\text{H}_2\text{O}_2] \\ \frac{d[\text{RS}]}{[W] \cdot dt} &= \left[0.081 \cdot k_{\text{Ph}} \cdot [\text{Ph}] - 1700 \cdot \exp\left(\frac{-5773}{T}\right) \cdot [\text{RS}] \right] \cdot [\text{H}_2\text{O}_2] \\ \frac{d[\text{CTL}]}{[W] \cdot dt} &= \left[0.095 \cdot k_{\text{Ph}} \cdot [\text{Ph}] - 6.7E8 \cdot \exp\left(\frac{-10344}{T}\right) \cdot [\text{CTL}] \right] \cdot [\text{H}_2\text{O}_2] \\ \frac{d[\text{BQ}]}{[W] \cdot dt} &= \left[0.344 \cdot k_{\text{Ph}} \cdot [\text{Ph}] - 3.6E6 \cdot \exp\left(\frac{-8420}{T}\right) \cdot [\text{BQ}] \right] \cdot [\text{H}_2\text{O}_2] \\ \frac{d[\text{MALE}]}{[W] \cdot dt} &= \left[(0.0019 \cdot k_{\text{Ph}} \cdot [\text{Ph}] + 0.186 \cdot k_{\text{CTL}} \cdot [\text{CTL}] - 1.0E9 \cdot \exp\left(\frac{-10945}{T}\right) \cdot [\text{MALE}]) \right] \cdot [\text{H}_2\text{O}_2] \\ \frac{d[\text{FUM}]}{[W] \cdot dt} &= \left[(0.0006 \cdot k_{\text{Ph}} \cdot [\text{Ph}] + 0.0191 \cdot k_{\text{HQ}} \cdot [\text{HQ}] + 0.0033 \cdot k_{\text{RS}} \cdot [\text{RS}] + 0.0001 \cdot k_{\text{BQ}} \cdot [\text{BQ}]) - 1.3E10 \cdot \exp\left(\frac{-12268}{T}\right) \cdot [\text{FUM}] \right] \cdot [\text{H}_2\text{O}_2] \\ \frac{d[\text{MALO}]}{[W] \cdot dt} &= \left[(0.0026 \cdot k_{\text{Ph}} \cdot [\text{Ph}] + 0.0232 \cdot k_{\text{RS}} \cdot [\text{RS}] + 0.0273 \cdot k_{\text{BQ}} \cdot [\text{BQ}]) - 200 \cdot \exp\left(\frac{-4931}{T}\right) \cdot [\text{MALO}] \right] \cdot [\text{H}_2\text{O}_2] \\ \frac{d[\text{OXA}]}{[W] \cdot dt} &= \left[(0.0945 \cdot k_{\text{RS}} \cdot [\text{RS}] - 3E12 \cdot \exp\left(\frac{-14073}{T}\right) \cdot [\text{OXA}]) \right] \cdot [\text{H}_2\text{O}_2] \\ \frac{d[\text{ACE}]}{[W] \cdot dt} &= [0.0075 \cdot k_{\text{Ph}} \cdot [\text{Ph}] + 0.163 \cdot k_{\text{HQ}} \cdot [\text{HQ}] + 0.0232 \cdot k_{\text{CTL}} \cdot [\text{CTL}] + 0.399 \cdot k_{\text{MALE}} \cdot [\text{MALE}]] \cdot [\text{H}_2\text{O}_2] \\ \frac{d[\text{FORM}]}{[W] \cdot dt} &= [0.0089 \cdot k_{\text{Ph}} \cdot [\text{Ph}] + 0.143 \cdot k_{\text{RS}} \cdot [\text{RS}] + k_{\text{MALO}} \cdot [\text{MALO}] + k_{\text{FUM}} \cdot [\text{FUM}]] \cdot [\text{H}_2\text{O}_2] \\ \frac{d[\text{CP}]}{[W] \cdot dt} &= 0.246 \cdot k_{\text{Ph}} \cdot [\text{Ph}] \cdot [\text{H}_2\text{O}_2] \end{aligned}$$

some uncertainty is associated to the maximum concentrations (5 and 1 mg/L, respectively). The activation energy values for acid by-products vary within the range of 41–117 kJ/mol, values in general higher than those obtained for the aromatics. Note the scarce oxidation of phenol to acids (the sum of the $S_{Ph \rightarrow acids}$ values in Table 2 is 2 mol%). Similar behavior was observed for *p*-benzoquinone while, on the other hand, around 20 mol% of dihydroxybenzenes are oxidized to acids.

A complex scheme reaction was first proposed for CP, which considered oxidative coupling reactions of phenol and aromatics:

$$\frac{d[CP]}{[W] \cdot dt} = \left(S_{Ph \rightarrow CP} \cdot k_{Ph} \cdot [Ph] + \sum_{arom.=1}^4 S_{arom \rightarrow CP} \cdot k_{arom} \cdot [arom] \right) \cdot [H_2O_2] \quad (11)$$

However, the integrated rate equation from (11) only fitted to the experimental data (Fig. 5) when $S_{arom \rightarrow PC} \approx 0$. The estimated concentration values are given in Fig. 5 (lines). The Fcriterion allows validating the model and the R^2 values are indicative of the good fit (Table 1). Therefore, phenol seems to be the only compound yielding oligomers (≈ 25 mol%) through oxidative coupling.

From the predicted time-course of phenol and its oxidation by-products (Figs. 1–5), the TOC evolution was derived and shown in Fig. 1 (lines). As can be seen, the calculated values are in good agreement with the experimental results. This result supports the proposed model.

The values of $S_{m \rightarrow CO_2}$, also collected in Table 2, were calculated as $100 - \sum S_{m \rightarrow n}$ (%), n being any by-product in the liquid phase. Note the direct mineralization of phenol ($S_{phenol \rightarrow CO_2} = 18.2\%$) and the important selectivity of aromatic intermediates towards mineralization ($S_{arom \rightarrow CO_2}$ values ranging from 73.6 to 97.3) instead of conversion into carboxylic acids, as typically considered in wet oxidation studies of phenol.

Taking into account these $S_{m \rightarrow CO_2}$ values (Table 2) and the kinetic expressions for phenol and its by-products (Eqs. 3–11), the production rate of CO_2 in amount of carbon evolved as CO_2 to gas phase per unit volume (L) of treated water (ppm carbon/L) can be expressed as follows:

$$\frac{d[TOC_{to}CO_2]}{[W] \cdot dt} = 18.2 \cdot r_{Phenol} + 73.6 \cdot r_{RS} + 79.1 \cdot r_{CTL} + 81.8 \cdot r_{HQ} + 97.3 \cdot r_{BQ} + 60 \cdot r_{MAL} + 100 \cdot r_{OXA} \quad (12)$$

The experimental concentration profiles (calculated as $TOC_0 - TOC_t$) and the simulated values (calculated by Eq. (12)) are shown in Fig. 7. The good correlation between both concentrations supports the reaction scheme.

Table 3 summarizes the complete kinetic model proposed for CWPO of phenol with the carbon black catalyst used. The validation of this model is illustrated by the parity plots of Fig. 8. The model also enables the prediction of the species time-course up to reaction times beyond the 6 h considered in the study (see profiles up to 24 h in Fig. S3 of Supporting Information).

3.3. Efficiency of H_2O_2 consumption

Hydrogen peroxide efficiency, calculated as the ratio of TOC to H_2O_2 conversion ($X_{TOC}/X_{H_2O_2}$), has been calculated at different operating conditions: $[W] = 2–12.5$ g/L, $T = 60–150^\circ C$. The results are given in Fig. 9. Both, catalyst concentration and temperature affect to the consumption of H_2O_2 . As can be seen, at high catalyst concentration (> 5 g/L), H_2O_2 -efficiency decreases from 100 to 80% after 3 h of reaction, and only at lower catalyst loads, 100% efficiency can be maintained upon reaction time, due to the presence of oxidizable intermediates at low conversion. Regarding reaction temperature, it is advisable working above $90^\circ C$ to achieve the highest efficiency at shorter reaction times.

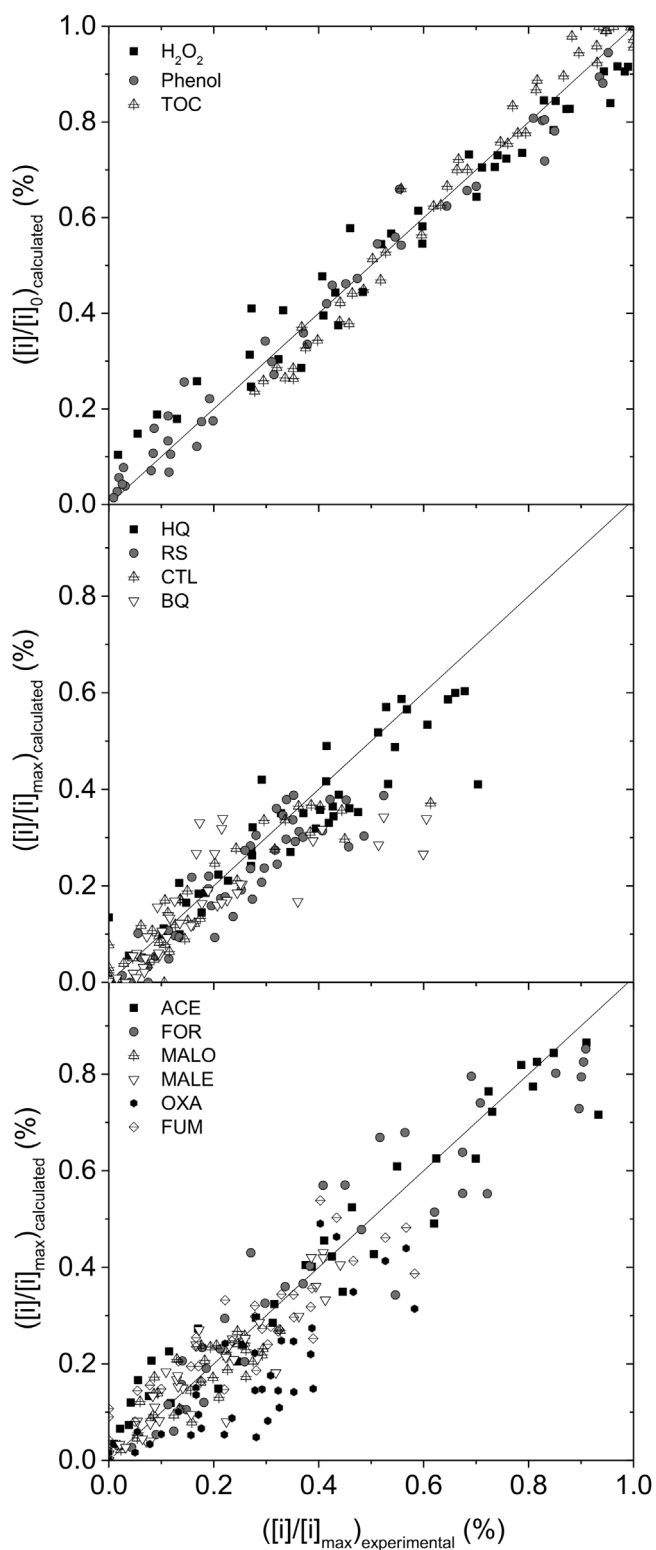


Fig. 8. Parity plots of normalized concentrations.

4. Conclusions

The CWPO process with a commercial carbon black as catalyst and using phenol as target pollutant is well-described by a set of power-law expressions with different reaction orders. The model predicts the phenol disappearance, hydrogen peroxide consumption and evolution of the individual aromatic intermediates and

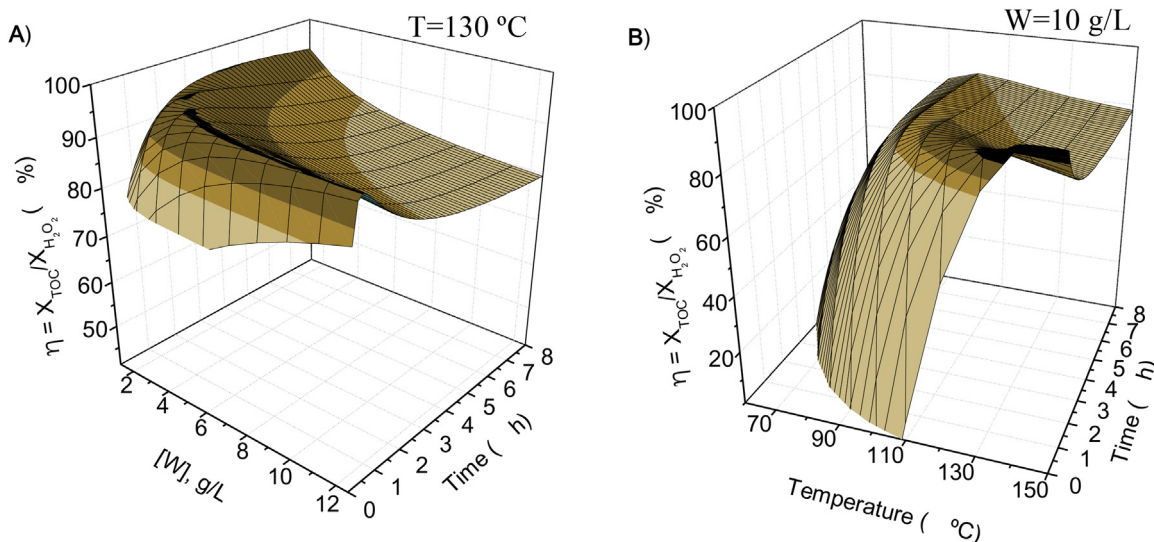


Fig. 9. Efficiency of H₂O₂ consumption (η) upon reaction time as a function of catalyst concentration (A) and temperature (B).

acid by-products (12 species in total) on the basis of the elucidated reaction pathway. The robustness of the model is demonstrated by the well prediction of the TOC and CO₂ evolution from the reaction rates of the model.

From the model arises that phenol oxidizes to aromatic intermediates (~55 mol%), and scarcely to short carboxylic acids (~2 mol%), mineralizes (~18 mol%) and also evolves to condensation by-products (~25 mol%) in parallel reactions. The resulting aromatic intermediates are mainly mineralized (~75–95 mol%) and in lower extent oxidized to carboxylic acids, they do not yield condensation products. Maleic, fumaric and malonic acids are further degraded to oxalic, acetic and formic, being the last two refractory to oxidation.

The model is valid at T < 130 °C and [W] < 10 g/L. More severe conditions would imply a greater contribution of the homogenous reaction, which was not considered in the model.

Acknowledgments

The authors wish to thank the Spanish MICINN for the financial support through the project CTQ2013-41963-R. The Comunidad Autónoma de Madrid is also acknowledged for financial support through the project S2013/MAE-2716. J.L. Díaz de Tuesta also acknowledges financial support to the Spanish MECD for the FPU grant.

Appendix A. Supplementary data

Supplementary data associated with this article can be found, in the online version, at <http://dx.doi.org/10.1016/j.apcatb.2017.03.031>.

References

- [1] S. Navalon, A. Dhakshinamoorthy, M. Alvaro, H. Garcia, Heterogeneous Fenton catalysts based on activated carbon and related materials, *ChemSusChem* 16 (12) (2011) 1712–1730.
- [2] G. Mezoegyi, F.P. van der Zee, J. Font, A. Fabregat, Towards advanced aqueous dye removal processes: a short review on the versatile role of activated carbon, *J. Environ. Manage.* 102 (2012) 148–164.
- [3] L.C.A. Oliveira, C.N. Silva, M.I. Yoshida, R.M. Lago, The effect of H₂ treatment on the activity of activated carbon for the oxidation of organic contaminants in water and the H₂O₂ decomposition, *Carbon* 42 (2004) 2279–2284.
- [4] V.P. Santos, M.F.R. Pereira, P.C.C. Faria, J.J.M. Orfao, Decolourisation of dye solutions by oxidation with H₂O₂ in the presence of modified activated carbons, *J. Hazard. Mater.* 162 (2009) 736–742.
- [5] H.T. Gomes, S.M. Miranda, M.J. Sampaio, A.M.T. Silva, J.L. Faria, Activated carbons treated with sulphuric acid: catalysts for catalytic wet peroxide oxidation, *Catal. Today* 151 (2010) 153–158.
- [6] F. Duarte, F.J. Maldonado-Hodar, L.M. Madeira, Influence of the characteristics of carbon materials on their behaviour as heterogeneous Fenton catalysts for the elimination of the azo dye Orange II from aqueous solutions, *Appl. Catal. B Environ.* 103 (2011) 109–115.
- [7] O. Türgay, G. Ersöz, S. Atalay, J. Forss, U. Welander, The treatment of azo dyes found in textile industry wastewater by anaerobic biological method and chemical oxidation, *Sep. Purif. Technol.* 79 (2011) 26–33.
- [8] H.T. Gomes, S.M. Miranda, M.J. Sampaio, J.L. Figueiredo, A.M. Silva, J.L. Faria, The role of activated carbons functionalized with thiol and sulfonic acid groups in catalytic wet peroxide oxidation, *Appl. Catal. B Environ.* 106 (2011) 390–397.
- [9] M. Soria-Sánchez, E. Castillejos-López, A. Maroto-Valiente, M. Pereira, J. Órfão, A. Guerrero-Ruiz, High efficiency of the cylindrical mesopores of MWCNTs for the catalytic wet peroxide oxidation of CI Reactive Red 241 dissolved in water, *Appl. Catal. B Environ.* 121 (2012) 182–189.
- [10] L. Gu, N. Zhu, H. Guo, S. Huang, S. Lou, H. Yuan, Adsorption and Fenton-like degradation of naphthalene dye intermediate on sewage sludge derived porous carbon, *J. Hazard. Mater.* 246–247 (2013) 145–153.
- [11] O. Pestunova, O. Ogorodnikova, V. Parmon, Studies on the phenol wet peroxide oxidation in the presence of solid catalysts, *Chem. Sustain. Dev.* 11 (2003) 227–232.
- [12] O. Taran, E. Polyanksaya, O. Ogorodnikova, V. Kuznetsov, V. Parmon, M. Besson, C. Descorme, Influence of the morphology and the surface chemistry of carbons on their catalytic performances in the catalytic wet peroxide oxidation of organic contaminants, *Appl. Catal. A Gen.* 387 (2010) 55–66.
- [13] R.S. Ribeiro, N.A. Fathy, A.A. Attia, A.M. Silva, J.L. Faria, H.T. Gomes, Activated carbon xerogels for the removal of the anionic azo dyes Orange II and Chromotrope 2R by adsorption and catalytic wet peroxide oxidation, *Chem. Eng. J.* 195 (2012) 112–121.
- [14] R.S. Ribeiro, A.M. Silva, J.L. Figueiredo, J.L. Faria, H.T. Gomes, Removal of 2-nitrophenol by catalytic wet peroxide oxidation using carbon materials with different morphological and chemical properties, *Appl. Catal. B Environ.* 140–141 (2013) 356–362.
- [15] C.M. Domínguez, P. Ocón, A. Quintanilla, J.A. Casas, J.J. Rodríguez, Graphite and carbon black materials as catalysts for wet peroxide oxidation, *Appl. Catal. B Environ.* 144 (2014) 599–606.
- [16] K. Rusevova, R. Koferstein, M. Rossel, H.H. Richnow, F.D. Kopinke, A. Georgi, LaFeO₃ and BiFeO₃ perovskites as nanocatalysts for contaminant degradation in heterogeneous Fenton-like reactions, *Chem. Eng. J.* 239 (2014) 322–331.
- [17] V. Subbaramaiah, V.Ch. Srivastava, I.D. Mallet, Catalytic wet peroxidation of pyridine bearing wastewater by cerium supported SBA-15, *J. Hazard. Mater.* 248–249 (2013) 355–363.
- [18] Q. Wang, S. Tian, P. Ning, Degradation mechanism of methylene blue in a heterogeneous fenton-like reaction catalyzed by ferrocene, *Ind. Eng. Chem. Res.* 53 (2) (2014) 643–649.
- [19] N. Inchaurreondo, P. Massa, R. Fenoglio, J. Font, P. Haure, Efficient catalytic wet peroxide oxidation of phenol at moderate temperature using a high-load supported copper catalyst, *Chem. Eng. J.* 198 (2012) 426–434.
- [20] T. Granato, F. Testa, R. Olivo, Catalytic activity of HKUST-1 coated on ceramic foam, *Microporous Mesoporous Mater.* 153 (2012) 236–246.
- [21] L. Xu, J. Wang, Magnetic nanoscaled Fe₃O₄/CeO₂ composite as an efficient fenton-like heterogeneous catalyst for degradation of 4-chlorophenol, *Environ. Sci. Technol.* 46 (18) (2012) 10145–10153.

[22] W. Luo, L. Zhu, N. Wang, H. Tang, M. Cao, Y. She, Efficient removal of organic pollutants with magnetic nanoscaled BiFeO₃ as a reusable heterogeneous fenton-like catalyst, *Environ. Sci. Technol.* 44 (5) (2010) 1786–1791.

[23] K. Hanna, T. Kone, C. Ruby, Fenton-like oxidation and mineralization of phenol using synthetic Fe(II)-Fe(III) green rusts, *Environ. Sci. Pollut. Res. Int.* 17 (1) (2010) 124–134.

[24] C. Bradua, L. Frunza, N. Mihalcea, S. Avramescu, M. Neață, I. Udrea, Removal of Reactive Black 5 azo dye from aqueous solutions by catalytic oxidation using CuO/Al₂O₃ and NiO/Al₂O₃, *Appl. Catal. B Environ.* 96 (3–4) (2010) 548–556.

[25] S. Caudo, Ch. Genovese, S. Perathoner, G. Centi, Copper-pillared clays (Cu-PILC) for agro-food wastewater purification with H₂O₂, *Microporous Mesoporous Mater.* 107 (2008) 46–57.

[26] C.M. Domínguez, A. Quintanilla, J.A. Casas, J.J. Rodríguez, Kinetics of wet peroxide oxidation of phenol with a gold/activated carbon catalyst, *Chem. Eng. J.* 253 (2014) 486–492.

[27] J. Guo, M. Al-Dahhan, Catalytic wet oxidation of phenol by hydrogen peroxide over pillared clay catalyst, *Ind. Eng. Chem. Res.* 42 (2003) 2450–2460.

[28] K.M. Valkaj, A. Katovic, S. Zrncevic, Investigation of the catalytic wet peroxide oxidation of phenol over different types of Cu/ZSM-5 catalyst, *J. Hazard. Mater.* 144 (2007) 663–667.

[29] S. Zrncevic, CWPO: an environmental solution for pollutant removal from wastewater, *Ind. Eng. Chem. Res.* 44 (2005) 6110–6114.

[30] X. Yang, P. Tian, X. Zhang, X. Yu, T. Wu, J. Xu, Y. Han, The generation of hydroxyl radicals by hydrogen peroxide decomposition on FeOCl/SBA-15 catalysts to phenol degradation, *AIChE J.* 61 (2015) 166–176.

[31] G.M. Eisenberg, Colorimetric determination of hydrogen peroxide, *Ind. Eng. Chem. Res.* 15 (1943) 327–328.

[32] J.A. Zazo, G. Pliego, S. Blasco, J.A. Casas, J.J. Rodriguez, Intensification of the fenton process by increasing the temperature, *Ind. Eng. Chem. Res.* 50 (2011) 866–870.

[33] J.A. Zazo, J.A. Casas, A.F. Mohedano, J.J. Rodríguez, Catalytic wet peroxide oxidation of phenol with a Fe/active carbon catalyst, *Appl. Catal. B Environ.* 65 (2006) 261–268.

[34] C.M. Domínguez, A. Quintanilla, J.A. Casas, J.J. Rodríguez, Highly efficient application of activated carbon as catalyst for wet peroxide oxidation, *Appl. Catal. B Environ.* 140–141 (2013) 663–670.

[35] M.E. Suarez-Ojeda, F. Stüber, A. Fortuny, A. Fabregat, J. Carrera, J. Font, *Appl. Catal. B Environ.* 58 (2005) 107.

[36] A. Quintanilla, M. Nieves, J. Tornero, J.A. Casas, J.J. Rodríguez, *Appl. Catal. B Environ.* 81 (2008) 105–114.

[37] T.M. Grant, C.J. King, *Carbon* 29 (1990) 264.

[38] E.Y. Osei-Twum, N.S. Abuzaid, G. Nahkla, *Bull. Environ. Contam. Toxicol.* 56 (1998) 513.

[39] A. Santos, P. Yustos, A. Quintanilla, F. García-Ochoa, J.A. Casas, J.J. Rodríguez, Evolution of toxicity upon wet catalytic oxidation of phenol, *Environ. Sci. Technol.* 38 (1) (2004) 133–138.